

Room-Temperature Phosphorescence Vapochromism through Conformational Control

Andrea Fermi,* Sapna Gahlot, Eric Jorand, Simone d'Agostino,* Yasi Dai, Fabrizia Negri,* Corinne Moustrou, Marc Gingras,* and Paola Ceroni



Cite This: *J. Am. Chem. Soc.* 2025, 147, 32309–32314



Read Online

ACCESS |

Metrics & More

Article Recommendations

Supporting Information

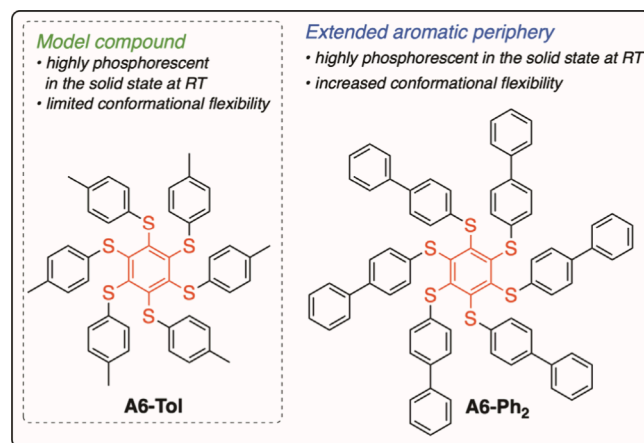
ABSTRACT: Solid-state room-temperature phosphorescence is rarely observed in organic molecules, and the modification of its color upon application of physical or chemical stimuli is hardly achieved. In this work, we demonstrate that a decorated persulfurated benzene shows reversible phosphorescence switching in the solid state, as a consequence of conformational changes induced by inclusion of solvent molecules. Quantum-chemical calculations suggest that the luminescence changes are due to emission from triplet states of different character. These results display the close relationship between structural factors and phosphorescence in solid state emitters, representing a valuable benchmark for the design of all-organic luminescent sensors with the desired photophysical properties.

Due to their countless applications in light generation,^{1–3} molecular and inorganic materials with tailored luminescent properties in the solid phase have been extensively studied in the last decades in crystal engineering.^{4,5} More recently, increasing attention has been devoted to materials able to show exalted room-temperature phosphorescence (RTP) in the solid state, a phenomenon most commonly detected in metal complexes.⁶ The same property is rather elusive for organic materials,^{7,8} since the population of the emitting triplet state cannot take advantage of heavy atoms able to induce spin-orbit coupling (SOC) and high intersystem crossing (ISC) rates.^{8,9} The design of organic materials showing high phosphorescence quantum yield in the solid phase is therefore limited by multiple chemical and structural factors, although the production could be achieved on a large scale (in contrast to their precious noble metal-based counterparts).^{5,10–13} As a consequence, the rational control of key luminescence parameters (i.e., energy, lifetime, quantum yield) is hardly realized, still making the development of stimuli-responsive organic triplet emitters highly challenging.^{14,15}

Arylthio-substituted persulfurated benzenes (such as **A6-Tol**, Scheme 1) represent an intriguing class of solid-state RTP emitters that we pioneered in 2013.^{16–22} While the relationship between their luminescent properties and structural factors (such as intramolecular conformation,^{13a,17} polymorphism,²⁰ aggregation^{18,23}) or physical stimuli (such as temperature¹⁷) have been described, the phosphorescence tuning via application of a chemical stimulus has not been observed within this class of compounds. Persulfurated benzenes and related compounds have also displayed intriguing properties as solid-state clathrates in the presence of solvent molecules,^{24–27} demonstrating their structural adaptability to the inclusion of several guests.

In light of these aspects and the results collected by our groups on per(phenylthio)benzenes,^{13a,16,17} we rationally designed simple materials based on a structural elongation

Scheme 1. Aryl-Substituted Persulfurated Benzenes Taken into Exam



for enhancing supramolecular interactions and for exhibiting reversible structure-dependent RTP in the presence of guest molecules. For this novel class of solid optical sensors, we selected simple biphenylthio arms to achieve a structural balance that maximizes phosphorescence and its effective control upon supramolecular inclusion.

Here, we describe how the phosphorescence of solid **A6-Ph₂** (Scheme 1) can be switched through the conformational change induced by the uptake of solvent molecules (i.e.,

Received: April 30, 2025

Revised: August 20, 2025

Accepted: August 20, 2025

Published: August 26, 2025



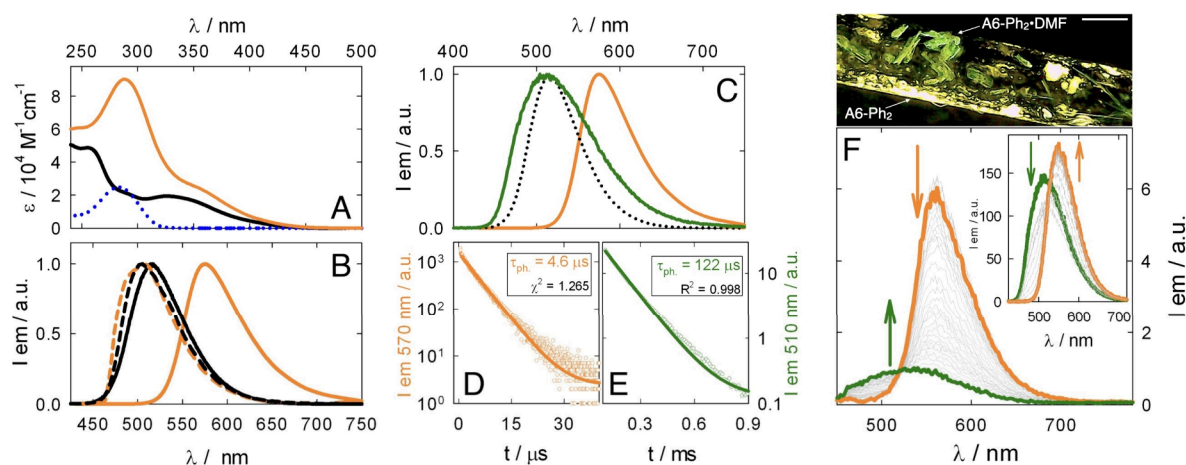


Figure 1. (A) Absorption spectra in CH_2Cl_2 at RT for **A6-Tol** (black line), **A6-Ph₂** (orange) and **Ph₂-SMe** (dotted line). (B) Normalized emission spectra of **A6-Tol** (black line) and **A6-Ph₂** (orange) in the solid state at RT and in a rigid matrix at 77 K (dashed lines; $\text{CH}_2\text{Cl}_2:\text{CH}_3\text{OH}$, 1:1 v/v). (C) Normalized emission spectra of solid **A6-Ph₂** (orange), **A6-Ph₂·DMF** (green), and **A6-Tol** (dotted line) at RT. (D, E) Emission decays for solid **A6-Ph₂** and **A6-Ph₂·DMF**, respectively, at RT. Monoexponential fitting curves are also shown. (F) Emission changes in solid **A6-Ph₂** upon exposure to DMF vapors at RT. Inset: reversible release of DMF molecules by solid **A6-Ph₂·DMF** in air. Top: micrograph of a glass pipette showing the phosphorescence of the pure and solvated form (scale bar: 1 mm). $340 < \lambda_{ex} < 380 \text{ nm}$.

Table 1. Photophysical Data Collected under Different Experimental Conditions

Compound	Absorption, CH_2Cl_2 , RT: λ (nm)/ ϵ ($\text{M}^{-1} \text{cm}^{-1}$)	Emission					
		solid, RT			$\text{CH}_2\text{Cl}_2:\text{CH}_3\text{OH}$ (1:1, v/v), 77 K		
		λ_{max} (nm)	τ (μs)	Φ	λ_{max} (nm)	τ (ms)	Φ
A6-Tol ^a	328/19400	517	3.0	1.0	505	4.0	1.0
Ph₂-SMe	283/24800	not luminescent			495 ^b	214 ^b	n.d.
A6-Ph₂	343/27700	575	4.6	0.8	510	7.5	1.0
A6-Ph₂·DMF		504	122	n.d. ^c			

^aData from ref 17. ^bPhosphorescence data. ^cData not determined due to the instability of the samples.

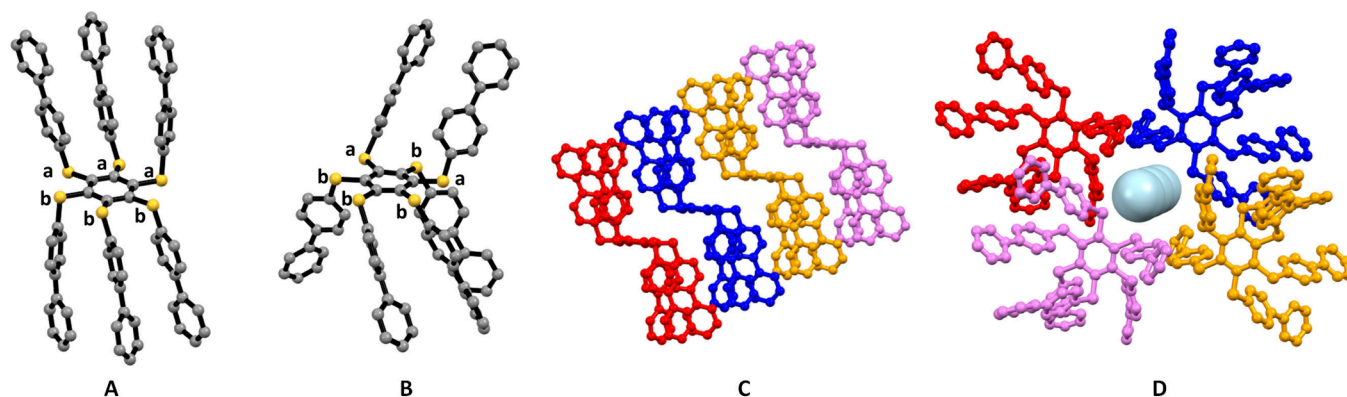


Figure 2. Molecular structures of **A6-Ph₂** (A) and **A6-Ph₂·X** (B), as determined from SC-XRD. Letters in lowercase indicate the orientations of the peripheral substituents with respect to the central benzene unit (a: above; b below; solvent molecules are not shown). C: columnar stacking detected in **A6-Ph₂**. D: solvent pocket in **A6-Ph₂·X** formed by four adjacent molecules, with solvent molecules shown as light-blue spheres; H_{CH} is omitted for clarity.

vapochromism^{28,29}), a property that has been exclusively observed for inorganic phosphors at RT.^{30–32}

We therefore present a class of fully organic, phosphorescent stimuli-responsive materials, obtained through simple and scalable protocols, thus demonstrating a new approach for solid-state optical sensing devices based on the rational control of intramolecular conformations.

Compound **A6-Ph₂** can be prepared through nucleophilic aromatic substitutions onto perhalogenobenzene, in the presence of an excess arylthiols and a base (e.g., K_2CO_3 , t -

BuOK , or NaH) in polar aprotic solvents, such as DMF (see the Supporting Information, SI).^{17,25,33,34}

The profile of the absorption spectrum of compound **A6-Ph₂** in CH_2Cl_2 between ca. 340 and 450 nm is similar to that recorded for model compound **A6-Tol**,¹⁶ while a major peak attributed to parent **Ph₂-SMe** is detected at 288 nm (Figure 1A and Figure S11). The increase in the extension of the peripheral π -system is therefore not significantly affecting the energy of the lowest-lying electronic transition. The same considerations hold by taking into account the luminescence

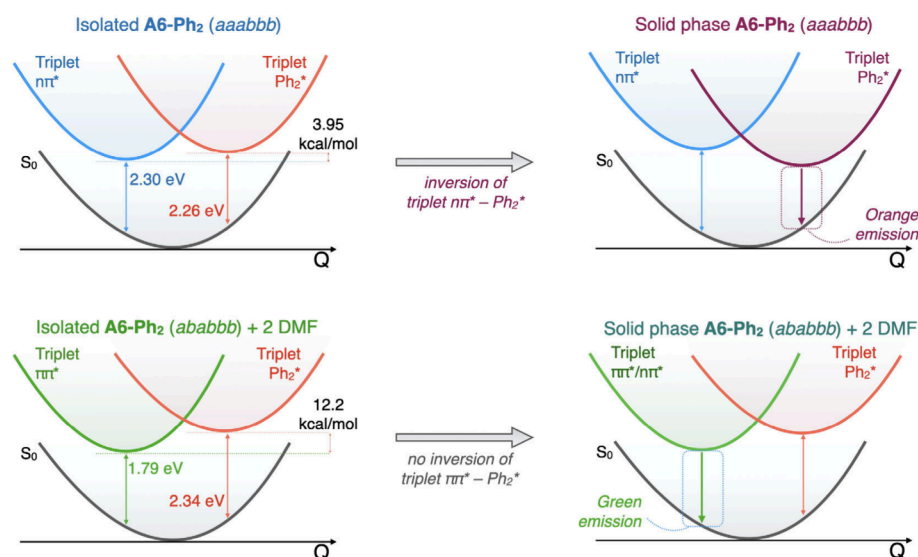


Figure 3. Schematic representation of the calculated potential energy profiles vs. the multidimensional displacement coordinate for the triplet excited states ($n\pi^*/\pi\pi^*$ and Ph_2^* character) of **A6-Ph₂** (top: *aaabbb*; bottom: *ababbb*) as isolated/solvated molecules and as aggregates.

properties in diluted rigid matrix at 77 K, where the emission spectra of **A6-Tol** and **A6-Ph₂** share comparable profiles, lifetimes in the order of 10^{-3} s and emission quantum yield (Figure 1B and Table 1). Similarly to **A6-Tol**, no significant emission ($\Phi_{\text{em}} < 10^{-3}$) has been detected for **A6-Ph₂** in air-equilibrated or deoxygenated solutions at RT;¹⁶ this behavior can be ascribed to the efficient nonradiative deactivation of the excited state in low viscosity media at RT.^{35–40}

More interestingly, the luminescence of pure **A6-Ph₂** in the solid state at RT is remarkably different in respect to those usually observed for similar derivatives, such as **A6-Tol**.^{16,17} the emission of **A6-Ph₂** is significantly red-shifted, peaking at $\lambda_{\text{max}} = 575$ nm (Figure 1B). Such changes have been rarely observed for this class of compounds²⁰ or for sulfurated derivatives of dicyanobenzene.^{41,42} Importantly, the emission lifetime ($\tau_{\text{ph.}} = 4.6$ μs ; Figure 1D) indicates radiative deactivation of a triplet excited state at RT. The remarkable emission quantum yield ($\Phi_{\text{ph.}} = 0.8$) makes compound **A6-Ph₂** another attractive example of an RT organic solid-state emitter within this family of compounds.

Comparison between absorption and excitation spectra collected from solid samples of **A6-Tol** and **A6-Ph₂** (Figure S13A,B) shows a significant shift to higher wavelengths for the latter. This aspect remarks differences in the absorption energies of the solid phases that are often attributable to structural factors, such as packing geometry, arrangements, and molecular conformation adopted in their crystal lattices.⁵

The structural analysis of bright orange polycrystalline samples of **A6-Ph₂** was carried out through powder X-ray diffraction (PXRD). The six biphenylthio substituents attached to the benzene core reveal an *aaabbb* pattern (*a* and *b* indicating substituents positions above and below the plane of the central ring, respectively), resulting in a chairlike conformation (Figure 2A and Table S1).⁴³ No specific intermolecular interactions are observed in the lattice of **A6-Ph₂**; crystal cohesion is due to dispersion forces and by molecules packing mainly by shape factor,⁴⁴ i.e. interlocking themselves in a slipped columnar fashion (Figure 2C).

Importantly, we noticed that the crystalline materials obtained from DMF and dimethylacetamide (DMA) solutions

exhibited similar powder XRD diffraction patterns and distinct from those observed for the as-synthesized **A6-Ph₂** (Figure S7). The thermogravimetric analysis (TGA) on the crystals grown in DMF and DMA indicated the presence of approximately 2–3 solvent molecules per each **A6-Ph₂** (Figure S10), highlighting that the compound crystallizes as a clathrate, as observed in similar materials.²⁴ In contrast, TGA measurements on the as-synthesized material confirmed the absence of solvent molecules. Therefore, the crystalline materials could be formulated as **A6-Ph₂** in its solvent-free form and as **A6-Ph₂·X** (where X = DMF, DMA) when isolated as solvates. These observations were further validated by single crystal XRD analysis (SC-XRD, details in Table S1). Figure 2B displays the crystal structures as determined by SC-XRD data for **A6-Ph₂·X**: the substituents adopt an asymmetric conformation with an *ababbb* pattern.²⁰ The crystal packing in **A6-Ph₂·X** highlights how the arrangement of **A6-Ph₂** molecules allows solvent molecules to fit into pockets (Figure 2D), thanks to weak hydrogen bond interactions between aromatic CH moieties from **A6-Ph₂** molecules and O atoms from the solvent [$d(\text{CH}_{\text{ar}} \cdots \text{O}_{\text{C=O}}) = 3.282(8)–3.547(9)$ and $3.32(1)–3.56(2)$ Å for **A6-Ph₂·DMF** and **A6-Ph₂·DMA**, respectively]. Both **A6-Ph₂·X** clathrates tend to easily lose solvent molecules when exposed to air at RT, as indicated by TGA analysis (Figure S10). By warming above 150 °C the original nonsolvated phase **A6-Ph₂** is obtained, as confirmed by powder XRD analysis (Figure S7).

The structural differences introduced in the solvated **A6-Ph₂·X** crucially impact the luminescent properties: compared to the solvent-free form, the isolated crystals of **A6-Ph₂·X** show a greenish phosphorescence reminiscent of model compound **A6-Tol** (Figure 1C and Table 1). The corresponding lifetime ($\tau_{\text{ph.}} = 122$ μs , Figure 1E) indicates phosphorescence emission from the solvated material.

A6-Ph₂ was thus employed in vapochromism tests, monitoring luminescence changes upon exposure to solvent vapors (details in SI). When the solvent-free form was exposed to DMF vapors, an increase in emission intensity around 505 nm was detected, accompanied by the substantial decrease of the original emission. This trend highlights the conversion of

the pure form to **A6-Ph₂·DMF** (Figure 1F). Remarkably, the changes observed in the photophysical behavior are reversible: upon exposure to air, the so-obtained **A6-Ph₂·DMF** releases DMF molecules, restoring the original phosphorescence signal of solvent-free **A6-Ph₂** (Figure 1F, inset). Hence, solid compound **A6-Ph₂** can reversibly convert its phosphorescence emission as a consequence of the conformational changes induced by the inclusion/release of DMF molecules. On the other hand, such behavior has not been observed with chlorinated solvents such as CH₂Cl₂ and CHCl₃ or with aromatic C₆H₆ (see Figure S20). Differences between the phosphorescence profiles of the pure and solvated forms are observed as well at low temperatures (Figure S15 and Table S2), indicating that the structural parameters of the two forms are not significantly affected upon increasing the rigidity of the lattice.

To understand the red-shifted emission of the solvent-free **A6-Ph₂** crystal compared to its solvated form, we performed quantum-chemical calculations on the isolated *aaabbb* and *ababbb* conformers as well as their corresponding aggregates. At the optimized ground-state geometry, the lowest triplet state of **A6-Ph₂** *aaabbb* has a dominant $n\pi^*$ nature, while **A6-Ph₂** *ababbb* is predominantly $\pi\pi^*$.

At higher energies, another triplet state with a localized excitation on biphenyl branches emerges (hereafter indicated as Ph₂^{*} character, Table S4). Specifically, in isolated **A6-Ph₂**, geometry optimization of the Ph₂^{*} triplet state places its emission energy at 2.26 eV, and its minimum 3.95 kcal/mol above the $n\pi^*$ state in the *aaabbb* conformation, while it appears 12.2 kcal/mol above the $\pi\pi^*$ in *ababbb* including two explicit DMF solvent molecules (Figure 3). Triplet-state geometry optimization predicts an **A6-Ph₂** *aaabbb* emission energy from the $n\pi^*$ triplet of 2.30 eV, similar to that of **A6-Tol** (2.32 eV, Table S5), contradicting experimental data (Figure 1).^{13a} Investigations on dimer and trimer aggregates of conformer *aaabbb* of **A6-Ph₂** do not evidence excitonic interactions, while they suggest an inversion between the $n\pi^*$ and the Ph₂^{*} triplet states (Figure 3 and Table S6). Similarly, QM/MM calculations suggest that this inversion takes place only in the *aaabbb* conformer (solvent-free crystals) and not in the *ababbb* conformer (solvated **A6-Ph₂**), as a result of the closer packing of **A6-Ph₂** molecules in the former (Figure 3 and Table S7, SI).

To investigate the reversible conformational change between the solvent-free and solvated crystals, we conducted molecular dynamics (MD) simulations (SI). Our results confirmed that conformational transitions in **A6-Ph₂** molecules, combined with the voids originated by the release of solvent molecules, led to the formation of different conformers during MD runs of up to 20 ns. Although this time scale is too short to definitively capture the *ababbb*-to-*aaabbb* transition observed for **A6-Ph₂**—particularly given the influence of the solvent—these results strongly support the reversibility of the conformational changes.

Overall, these findings demonstrate a rationale to design semiflexible persulfurated benzenes and to achieve stimuli-responsive RTP material in the solid state, without using noble metal complexes. Inclusion of solvent molecules leads to significant conformational changes that affect the emission color and photophysical properties. Importantly, the vapochromic behavior at RT is indubitably accompanied by the reversible conversion between two conformations. Calculations suggest that the observed vapochromism is associated with a

triplet emission that reflects the different nature of the two conformers: the red-shifted emission originates from the Ph₂^{*} triplet state of *aaabbb* conformers in solvent-free **A6-Ph₂**, while the core centered $\pi\pi^*$ state is responsible for emission in the solvated crystal, as observed in **A6-Tol** and similar derivatives. Thus, we open new avenues for the design of novel and scalable all-organic sensing devices and optoelectronic materials that are highly effective in the solid state by RTP.

■ ASSOCIATED CONTENT

Supporting Information

The Supporting Information is available free of charge at <https://pubs.acs.org/doi/10.1021/jacs.5c07339>.

Synthetic details, XRD data, thermogravimetric analysis, photophysical characterization, and computational details (PDF)

Accession Codes

Deposition Numbers 2443649–2443651 contain the supplementary crystallographic data for this paper. These data can be obtained free of charge via the joint Cambridge Crystallographic Data Centre (CCDC) and Fachinformationszentrum Karlsruhe Access Structures service.

■ AUTHOR INFORMATION

Corresponding Authors

Andrea Fermi – Dipartimento di Chimica “Giacomo Ciamician”, Alma Mater Studiorum–Università di Bologna, 40129 Bologna, Italy; orcid.org/0000-0003-1080-0530; Email: andrea.fermi2@unibo.it

Simone d’Agostino – Dipartimento di Chimica “Giacomo Ciamician”, Alma Mater Studiorum–Università di Bologna, 40129 Bologna, Italy; orcid.org/0000-0003-3065-5860; Email: simone.dagostino2@unibo.it

Fabrizia Negri – Dipartimento di Chimica “Giacomo Ciamician”, Alma Mater Studiorum–Università di Bologna, 40129 Bologna, Italy; orcid.org/0000-0002-0359-0128; Email: fabrizia.negri@unibo.it

Marc Gingras – Aix-Marseille Université, CNRS, 13288 Marseille, France; orcid.org/0000-0003-3704-7024; Email: marc.gingras@univ-amu.fr

Authors

Sapna Gahlot – Aix-Marseille Université, CNRS, 13288 Marseille, France

Eric Jorand – Aix-Marseille Université, CNRS, 13288 Marseille, France

Yasi Dai – Dipartimento di Chimica “Giacomo Ciamician”, Alma Mater Studiorum–Università di Bologna, 40129 Bologna, Italy; orcid.org/0000-0002-4508-7547

Corinne Moustrou – Aix-Marseille Université, CNRS, 13288 Marseille, France

Paola Ceroni – Dipartimento di Chimica “Giacomo Ciamician”, Alma Mater Studiorum–Università di Bologna, 40129 Bologna, Italy; orcid.org/0000-0001-8916-1473

Complete contact information is available at: <https://pubs.acs.org/doi/10.1021/jacs.5c07339>

Author Contributions

The manuscript was written through contributions of all authors. All authors have given approval to the final version of the manuscript.

Funding

M.G. is grateful to the Agence Nationale de la Recherche (ANR) in France (program PRC) for the grant ANR-20-CE07-0031 Acronym: "SulfurDance" and financial support from the Excellence Initiative of Aix-Marseille University – A*Midex, a French "Investissements d'Avenir" program, and a doctoral contract to S.G. A.F. is grateful to the European Union – Next Generation EU under the National Recovery and Resilience Plan (PNRR M4 C2 Investment 1.1, Notice Prin 2022 - DD N. 1409 14/09/2022, title "Engineering LIGHT-activated materials for the abatement of ENvironmentally hazardous and pollutiNG substances" (ENLIGHTENING), sector PE4, proposal code P2022PZ2MM - CUP J53D23014600001. F.N. acknowledges the European Union – Resilience Plan (PNRR M4C2, Investment 1.4 – Call for tender n. 3138 dated 16/12/2021 – CN00000013 National Centre for HPC, Big Data and Quantum Computing (HPC) – CUP J33C22001170001).

Notes

The authors declare no competing financial interest.

ACKNOWLEDGMENTS

The University of Bologna is gratefully acknowledged by A.F., S.d.A., P.C., and F.N. Aix-Marseille Université, CINaM and CNRS France are thanked by M.G.

REFERENCES

- (1) Xu, H.; Chen, R.; Sun, Q.; Lai, W.; Su, Q.; Huang, W.; Liu, X. Recent Progress in Metal-Organic Complexes for Optoelectronic Applications. *Chem. Soc. Rev.* **2014**, *43* (10), 3259–3302.
- (2) Mao, L.; Wu, Y.; Stoumpos, C. C.; Wasielewski, M. R.; Kanatzidis, M. G. White-Light Emission and Structural Distortion in New Corrugated Two-Dimensional Lead Bromide Perovskites. *J. Am. Chem. Soc.* **2017**, *139* (14), 5210–5215.
- (3) Ostroverkhova, O. Organic Optoelectronic Materials: Mechanisms and Applications. *Chem. Rev.* **2016**, *116* (22), 13279–13412.
- (4) Xu, S.; Duan, Y.; Liu, B. Precise Molecular Design for High-Performance Luminogens with Aggregation-Induced Emission. *Adv. Mater.* **2020**, *32* (1), 1903530.
- (5) Gierschner, J.; Shi, J.; Milián-Medina, B.; Roca-Sanjuán, D.; Varghese, S.; Park, S. Luminescence in Crystalline Organic Materials: From Molecules to Molecular Solids. *Adv. Opt. Mater.* **2021**, *9* (13), 2002251.
- (6) Ravotto, L.; Ceroni, P. Aggregation Induced Phosphorescence of Metal Complexes: From Principles to Applications. *Coord. Chem. Rev.* **2017**, *346*, 62–76.
- (7) Mukherjee, S.; Thilagar, P. Recent Advances in Purely Organic Phosphorescent Materials. *Chem. Commun.* **2015**, *51* (55), 10988–11003.
- (8) Zhao, W.; He, Z.; Tang, B. Z. Room-Temperature Phosphorescence from Organic Aggregates. *Nat. Rev. Mater.* **2020**, *5* (12), 869–885.
- (9) Partanen, I.; Al-Saedy, O.; Eskelinen, T.; Karttunen, A. J.; Saarinen, J. J.; Mrózek, O.; Steffen, A.; Belyaev, A.; Chou, P.; Koshevoy, I. O. Fast and Tunable Phosphorescence from Organic Ionic Crystals. *Angew. Chem.* **2023**, *135* (36), No. e202305108.
- (10) Kwon, M. S.; Yu, Y.; Coburn, C.; Phillips, A. W.; Chung, K.; Shanker, A.; Jung, J.; Kim, G.; Pipe, K.; Forrest, S. R.; Youk, J. H.; Gierschner, J.; Kim, J. Suppressing Molecular Motions for Enhanced Room-Temperature Phosphorescence of Metal-Free Organic Materials. *Nat. Commun.* **2015**, *6* (1), 8947.
- (11) d'Agostino, S.; Spinelli, F.; Taddei, P.; Ventura, B.; Grepioni, F. Ultralong Organic Phosphorescence in the Solid State: The Case of Triphenylene Cocrystals with Halo- and Dihalo-Penta/Tetrafluorobenzene. *Cryst. Growth Des.* **2019**, *19* (1), 336–346.
- (12) Azzali, A.; d'Agostino, S.; Capacci, M.; Spinelli, F.; Ventura, B.; Grepioni, F. Assembling Photoactive Materials from Polycyclic Aromatic Hydrocarbons (PAHs): Room Temperature Phosphorescence and Excimer-Emission in Co-Crystals with 1,4-Diiodotetrafluorobenzene. *CrystEngComm* **2022**, *24* (32), 5748–5756.
- (13) (a) Fermi, A.; d'Agostino, S.; Dai, Y.; Brunetti, F.; Negri, F.; Gingras, M.; Ceroni, P. Unravelling the Role of Structural Factors in the Luminescence Properties of Persulfurated Benzenes. *Chem. Eur. J.* **2024**, *30* (43), No. e202401768. (b) Wagalgave, S. M.; Kongasseri, A. A.; Singh, U.; Anilkumar, A.; Ansari, S. N.; Pati, S. K.; George, S. J. Core-Substituted Pyromellitic Diimides: A Versatile Molecular Scaffold for Tunable Triplet Emission. *J. Am. Chem. Soc.* **2025**, *147* (18), 15591–15601. (c) Sun, H.; Li, X.; Hsu, C.-H.; Hung, C.-M.; Wu, B.; Su, Z.-H.; Baryshnikov, G. V.; Li, C.; Ågren, H.; Zhang, Z.; Huang, W.; Wu, D.; Chou, P.-T.; Zhu, L. Sulfur Lone Pairs Open Avenues for $\pi^* \rightarrow n$ Orange-to-Red TADF and OLEDs. *J. Am. Chem. Soc.* **2025**, *147* (6), 5432–5439.
- (14) Tani, Y.; Terasaki, M.; Komura, M.; Ogawa, T. Room-Temperature Phosphorescence-to-Phosphorescence Mechanochromism of a Metal-Free Organic 1,2-Diketone. *J. Mater. Chem. C* **2019**, *7* (38), 11926–11931.
- (15) Komura, M.; Ogawa, T.; Tani, Y. Room-Temperature Phosphorescence of a Supercooled Liquid: Kinetic Stabilisation by Desymmetrisation. *Chem. Sci.* **2021**, *12* (43), 14363–14368.
- (16) Bergamini, G.; Fermi, A.; Botta, C.; Giovannella, U.; Di Motta, S.; Negri, F.; Peresutti, R.; Gingras, M.; Ceroni, P. A Persulfurated Benzene Molecule Exhibits Outstanding Phosphorescence in Rigid Environments: From Computational Study to Organic Nanocrystals and OLED Applications. *J. Mater. Chem. C* **2013**, *1* (15), 2717–2724.
- (17) Fermi, A.; Bergamini, G.; Peresutti, R.; Marchi, E.; Roy, M.; Ceroni, P.; Gingras, M. Molecular Asterisks with a Persulfurated Benzene Core Are among the Strongest Organic Phosphorescent Emitters in the Solid State. *Dyes Pigment.* **2014**, *110*, 113–122.
- (18) Fermi, A.; Bergamini, G.; Roy, M.; Gingras, M.; Ceroni, P. Turn-on Phosphorescence by Metal Coordination to a Multivalent Terpyridine Ligand: A New Paradigm for Luminescent Sensors. *J. Am. Chem. Soc.* **2014**, *136* (17), 6395–6400.
- (19) Villa, M.; Roy, M.; Bergamini, G.; Gingras, M.; Ceroni, P. A Turn-on Phosphorescent Sensor of Pb²⁺ in Water by the Formation of a Coordination Polymer. *Dalt. Trans.* **2019**, *48* (12), 3815–3818.
- (20) Wu, H.; Baryshnikov, G. V.; Kuklin, A.; Minaev, B. F.; Wu, B.; Gu, L.; Zhu, L.; Ågren, H.; Zhao, Y. Multidimensional Structure Conformation of Persulfurated Benzene for Highly Efficient Phosphorescence. *ACS Appl. Mater. Interfaces* **2021**, *13* (1), 1314–1322.
- (21) Jia, X.; Shao, C.; Bai, X.; Zhou, Q.; Wu, B.; Wang, L.; Yue, B.; Zhu, H.; Zhu, L. Photoexcitation-Controlled Self-Recoverable Molecular Aggregation for Flicker Phosphorescence. *Proc. Natl. Acad. Sci. U. S. A.* **2019**, *116* (11), 4816–4821.
- (22) Hayduk, M.; Riebe, S.; Voskuhl, J. Phosphorescence Through Hindered Motion of Pure Organic Emitters. *Chem. Eur. J.* **2018**, *24* (47), 12221–12230.
- (23) (a) Shen, S.; Baryshnikov, G. V.; Xie, Q.; Wu, B.; Lv, M.; Sun, H.; Li, Z.; Ågren, H.; Chen, J.; Zhu, L. Making Multi-Twisted Luminophores Produce Persistent Room-Temperature Phosphorescence. *Chem. Sci.* **2023**, *14* (4), 970–978. (b) Zhang, B.; Li, B.; Zhang, H.; Ma, B.; Lou, J.; Dong, X.; Yang, D.; Tang, B. Z.; Wang, Z. New Wine in Old Bottles: Fully Substituted Arylthio Effect Realizes High-Efficiency Purely Organic Phosphorescence Light-Emitting Diode With Single and Ultra-Stable Spectra Under 2000 cd m⁻². *Aggregate* **2025**, *6*, No. e726. (c) Gahlot, S.; Gradone, A.; Roy, M.; Giorgi, M.; Conti, S.; Ceroni, P.; Villa, M.; Gingras, M. Persulfurated Benzene-Cored Asterisks with π -Extended ThioNaphthyl Arms: Synthesis, Structural, Photophysical and Covalent Dynamic Properties. *Chem. Eur. J.* **2022**, *28* (46), No. e202200797. (d) Sun, H.; Zhou, L.; Gong, R.; Zhang, M.; Shen, S.; Liu, M.; Wang, C.; Xu, X.; Li, Z.; Cheng, J.; Chen, W.; Zhu, L. A Single Carbon-Dot System Enabling Multiple Stimuli Activated Room-Temperature Phosphorescence. *ACS Appl. Mater. Interfaces* **2023**, *15* (18), 22415–22425.

- (24) MacNicol, D. D.; Wilson, D. R. New Strategy for the Design of Inclusion Compounds: Discovery of the 'Hexa-Hosts'. *J. Chem. Soc., Chem. Commun.* **1976**, No. 13, 494–495.
- (25) Hardy, A. D. U.; MacNicol, D. D.; Wilson, D. R. A New Approach for the Design of Inclusion Compounds. *J. Chem. Soc. Perkin Trans. 2* **1979**, No. 7, 1011.
- (26) Gilmore, C. J.; MacNicol, D. D.; Mallinson, P. R.; Murphy, A.; Russell, M. A. Crystal Structure Analysis of the Carbon Tetrabromide Clathrate of Hexakis (Phenylseleno) Benzene. *J. Inclusion Phenom.* **1984**, *1* (1), 295–299.
- (27) Farrugia, L. J.; Gall, J. H.; MacNicol, D. D. 1,2,4,5-Tetrakis(Phenylsulfonyl)Benzene: A Novel Quadruped Host with D2 Symmetry Having Ordered Sulfolane and Cycloheptanone Guests. *Chem. Commun.* **2012**, *48* (86), 10600–10602.
- (28) Yamada, S.; Katsuki, A.; Nojiri, Y.; Tokugawa, Y. Vapochromism Associated with the Changes in the Molecular Arrangement of Organic Crystals. *CrystEngComm* **2015**, *17* (6), 1416–1420.
- (29) Reus, C.; Baumgartner, T. Stimuli-Responsive Chromism in Organophosphorus Chemistry. *Dalt. Trans.* **2016**, *45* (5), 1850–1855.
- (30) Wenger, O. S. Vapochromism in Organometallic and Coordination Complexes: Chemical Sensors for Volatile Organic Compounds. *Chem. Rev.* **2013**, *113* (5), 3686–3733.
- (31) Li, E.; Jie, K.; Liu, M.; Sheng, X.; Zhu, W.; Huang, F. Vapochromic Crystals: Understanding Vapochromism from the Perspective of Crystal Engineering. *Chem. Soc. Rev.* **2020**, *49* (5), 1517–1544.
- (32) Fermi, A. Conformation Dependent Room Temperature Phosphorescence in Organic Materials. *ChemPhotoChem.* **2025**, *9*, No. e202400404.
- (33) Tucker, J. H. R.; Gingras, M.; Brand, H.; Lehn, J.-M. Redox Properties of Polythiaarene Derivatives. A Novel Class of Electron Acceptors. *J. Chem. Soc. Perkin Trans. 2* **1997**, No. 7, 1303–1308.
- (34) Gingras, M.; Raimundo, J.; Chabre, Y. M. Persulfurated Aromatic Compounds. *Angew. Chem., Int. Ed.* **2006**, *45* (11), 1686–1712.
- (35) Mei, J.; Leung, N. L. C.; Kwok, R. T. K.; Lam, J. W. Y.; Tang, B. Z. Aggregation-Induced Emission: Together We Shine, United We Soar! *Chem. Rev.* **2015**, *115* (21), 11718–11940.
- (36) Zhang, H.; Zheng, X.; Xie, N.; He, Z.; Liu, J.; Leung, N. L. C.; Niu, Y.; Huang, X.; Wong, K. S.; Kwok, R. T. K.; Sung, H. H. Y.; Williams, I. D.; Qin, A.; Lam, J. W. Y.; Tang, B. Z. Why Do Simple Molecules with "Isolated" Phenyl Rings Emit Visible Light? *J. Am. Chem. Soc.* **2017**, *139* (45), 16264–16272.
- (37) Würthner, F. Aggregation-Induced Emission (AIE): A Historical Perspective. *Angew. Chem., Int. Ed.* **2020**, *59* (34), 14192–14196.
- (38) Suman, G. R.; Pandey, M.; Chakravarthy, A. S. J. Review on New Horizons of Aggregation Induced Emission: From Design to Development. *Mater. Chem. Front.* **2021**, *5* (4), 1541–1584.
- (39) Sturala, J.; Etherington, M. K.; Bismillah, A. N.; Higginbotham, H. F.; Trewby, W.; Aguilar, J. A.; Bromley, E. H. C.; Avestro, A.-J.; Monkman, A. P.; McGonigal, P. R. Excited-State Aromatic Interactions in the Aggregation-Induced Emission of Molecular Rotors. *J. Am. Chem. Soc.* **2017**, *139* (49), 17882–17889.
- (40) Sussardi, A. N.; Turner, G. F.; Richardson, J. G.; Spackman, M. A.; Turley, A. T.; McGonigal, P. R.; Jones, A. C.; Moggach, S. A. Tandem High-Pressure Crystallography-Optical Spectroscopy Unpacks Noncovalent Interactions of Piezochromic Fluorescent Molecular Rotors. *J. Am. Chem. Soc.* **2023**, *145* (36), 19780–19789.
- (41) Riebe, S.; Vallet, C.; van der Vight, F.; Gonzalez-Abra delo, D.; Wölper, C.; Strassert, C. A.; Jansen, G.; Knauer, S.; Voskuhl, J. Aromatic Thioethers as Novel Luminophores with Aggregation-Induced Fluorescence and Phosphorescence. *Chem. Eur. J.* **2017**, *23* (55), 13660–13668.
- (42) Schmiedtchen, M.; Maisuls, I.; Wölper, C.; Strassert, C. A.; Voskuhl, J. Regioisomers of Aromatic Thioethers with Aggregation-Induced Phosphorescence. *ChemPhotoChem.* **2024**, *8* (2), No. e202300209.
- (43) Villa, M.; d'Agostino, S.; Sabatino, P.; Noel, R.; Busto, J.; Roy, M.; Gingras, M.; Ceroni, P. Pentasulfurated Benzene-Cored Asterisks: Relationship between Crystal Structure and Luminescence Properties. *New J. Chem.* **2020**, *44* (8), 3249–3254.
- (44) Braga, D.; d'Agostino, S.; Grepioni, F. Shape Takes the Lead: Templating Organic 3D-Frameworks around Organometallic Sandwich Compounds. *Organometallics* **2012**, *31* (5), 1688–1695.